Revista Mexicana de Física **41**, *No. 2 (1995) 147–180*

Quantum-statistical approach to dynamic problems of solid mechanics

ALEXANDER S. BALANKIN
Instituto Tecnológico y de Estudios Superiores de Monterrey
Campus Estado de México, México

Recibido el 19 de agosto de 1994; aceptado el 3 de enero de 1995

ABSTRACT. The present article reviews a quantum-statistical approach to dynamic problems in solid mechanics, when macroscopic defects, nucleation and propagation are not decisive in the irreversible deformation and fracture of a solid. The basic principles to construct quantum and quantum-statistical models of an irreversible deformed or fractured solid are discussed. A general quantum-statistical model of irreversible deformations and fracture of a solid under dynamic (shocking) loading is considered. The connection between the quantum-statistical approach and fractal solid mechanics is discussed. It is shown that the quantum-statistical approach is useful for an adequate description of various behavior patterns and fracture phenomena in irreversible deformed solid under dynamic loading. Some future research trends in this area are suggested as well as potential applications in basic and applied research.

RESUMEN. En el presente artículo se revisa un enfoque estadístico cuántico de problemas dinámicos en mecánica de sólidos, para el caso cuando la nucleación de defectos macroscópicos y su propagación no son relevantes en la fractura y la deformación irreversible de un sólido. Se discuten los principios básicos que permiten construir modelos cuánticos y estadístico-cuánticos de la fractura de sólidos, y sólidos deformados de manera irreversible. Se considera un modelo general cuántico-estadístico de la deformación irreversible y la fractura de un sólido bajo condiciones de carga dinámica (impacto). Se discute la conexión que existe entre el enfoque cuántico-estadístico y la mecánica fractal de sólidos. Se muestra que el enfoque cuántico-estadístico es útil para describir adecuadamente varios tipos de deformación y fenómenos de fractura de sólidos deformados de manera irreversible bajo condiciones de cargas dinámicas. En esta área se sugieren algunas tendencias de investigación a futuro, así como aplicaciones potenciales en investigación básica y aplicada.

PACS: 05.30; 05.70: 62.20

1. INTRODUCTION

The relationship between the structural parameters of a material and its dynamic strength is displayed largely under conditions when (in contrast to the quasi-static loading) the influence of defect nucleation and propagation is not decisive in the deformation and fracture of solids [1,2]. In particular, such conditions are created by high velocity impact, or shock loading, when the rate of loading is higher than that of defect propagation [2–6]. Irreversible dynamic deformations and fracture of solids under such loading belong to the class of processes in which a complex behavior at the microscopic level is behind the macroscopic effects [1,2,4]. The stability of real structures that operate under complex conditions, therefore, can be predicted reliably only with a clear understanding of the nature and kinetics of the quantum processes in a deformed solid [7–9]. The nature of

the relations between processes of different scales constitute the central problem in solid mechanics [1,10–12].

As noted in Ref. [13], at present, a theory of deformed solid similar to quantum physics or chemistry is urgently required. Such a theory would make it possible to calculate the physicomechanical properties of materials using only their fundamental physical parameters and to answer briefly the following questions: What is the nature of a given crystal: brittle, plastic, or superplastic? What is the mechanism of irreversible deformation and propagation of microcracks in a given crystal under the monotonic loading and unloading, under the dynamic loading, under the cyclic loading, under the stationary loading over a long period of time, or at elevated temperature, etc.?

Traditionally, the analysis of processes that control plastic deformation and fracture of solids at the microlevel has been confined to consideration of models that take into account only paired interatomic bonds [7,8,13–15].

At the same time, strong correlation of the relative positions of atoms at distances that significantly exceed the interatomic distances —a correlation that ensures the shear stability of solids— is characteristic of states of condensed matter [1,2]. Therefore, the rheological behavior of solids is determined by the dynamics of collective excitations induced by an external factor [1]. Thus plastic deformation and fracture are collective, far-from-equilibrium processes, whose kinetics are governed by the self-organization of dissipative structures that ensure an optimal (for specified loading) level of dissipation of energy of an external action (see, for example Refs.[1,2,16]). Therefore, in developing a physical theory of the dynamic strength of solids it is necessary to exhibit the mechanisms of microscopic processes limiting the defect dynamics, because it is this which determines the process of plastic deformation of a solid.

The difficulties encountered in theoretical and experimental investigations of the dynamic behavior of microscopic defects are due to the great variety of factors influencing their mobility. Furthermore, any physicomechanical action moves a deformed solid away from a state of the thermodynamic equilibrium [1]. In turn, as a consequence of shear stability, in a nonhydrostatically stressed solid, the additivity property of energy and entropy (the latter begins to depend on the shape of the body) is violated. Thus, the response of a solid is determined by the processes of entropy production and energy redistribution, both within the solid and between the deformed body and the surrounding medium. Notice, that a deformed solid as a whole is by nature, a thermodynamically closed system (except for some special cases) for which the corresponding formulations of the laws of thermodynamics, the principle of Prigogine, the Clausius-Duhem relation, etc. are valid [1,2]. However, the approximation of a continuum is never strictly valid, because of the existence of nonuniform fluctuations in the density and shape even in the state of equilibrium [1,9–12]. In fact, in some cases these effects can be neglected, but generally, the space occupied by a deformed solid does not possess the homogeneity property. At the same time, for deformed solids, the property of scaling invariance should be valid [1,12,17–20]. It is the scaling invariance that provides the possibility of calculations of the macroscopic parameters of deformed solids on microscale [1,21–24].

A quantum-statistical approach to dynamic problems of solid mechanics was proposed in our works [24–26] (see also Refs. [1,25,16]). This review is focused on systematic account of the basic concepts and fundamental principles of this approach. The most important

results associated with shock loading and armor piercing, which were obtained by using quantum-statistical approach, are also discussed.

In this section, below, we consider same classical aspects of shock loading and high velocity penetration problems. In Sect. 2, the common principles of construction of quantum fracture mechanics models of a deformed solid are analyzed. As a result we conclude that real processes of plastic deformation and fracture of solid materials unusual from the point of view of quantum fracture models which are based on the consideration of pair wise interatomic potentials. In Sect. 3, general quantum-statistical model of a irreversible deformed solid is considered. The applications of this model to some problems of solid mechanics are briefly discussed. The fractal effects in phenomena of plastic deformation and fracture of a solid are also discussed. In Sect. 4, the advanced applications of quantum statistical model to the problem of irreversible deformations of a solid under shock loading is considered with respect of the results of the experimental investigations. In Sect. 5, we consider the results of application of quantum statistical model for derivation of microscopic expressions for parameters which governs the processes of armor piercing. The possibility of some other applications of the reviewed quantum statistical approach and the necessity of further study in this direction are emphasized in conclusion.

1.1 The shock loading problem

The problem of adequate description of the processes occurring in solid under impact (or shock) loading is of fundamental and applied importance. In this problem, as in any other dynamic problem, the main question concerns the forces that characterize motion, that is the forces that determine the dynamic strength of a material.

The overwhelming majority of physical phenomena are so complex that, even with the current state of science, one can rarely create a universal theory of one or another of them. A single course remains at the disposal of the investigator: *To experimentally identify the main parameters governing the phenomenon within their range of variation, abstracted from the less important parameters, and to construct the simplest possible model of the phenomenon, clearly revealing its physical essence, for the conditions under consideration.* Excellent example of a solution found using this methodological approach is the classical theory of shock waves.

It was shown that if macroscopic mass velocity of the atoms of a solid, u, is less than critical value u_E then the transverse and longitudinal elastic waves propagate through the solid with the velocities C_t and C_l correspondingly. The pressure in the elastic wave is

$$P = \rho C_l u < P_{\mathrm{HEL}} = \rho C_l u_E, \tag{1}$$

where P_{HEL} is the Hugoniot elastic limit [3,4,27].

However, when $u > u_E$ a shock wave develops, and energy of external action is localized in the front of shock wave, with velocity

$$D = C_0 + bu, \qquad C_0 = \sqrt{\frac{B}{\rho}} \leq C_l, \tag{2}$$

where b is a constant of a material [27–29].

If $D < C_l$ shock wave has a two-wave structure with the *elastic precursor* which moves with the longitudinal wave velocity $C_l > D$. Mass velocity in the front of the elastic precursor is constant u_E [29]. The macroscopic structure of the shock has been studied thoroughly in terms of phenomenological models (see, for example, Refs. [6,27–30]).

The quantum-statistical model of deformation of a solid under shock loading was developed in our works [24–26]. The microscopic expressions for the parameters that determine the kinetics of the various regimes of shock propagation in solid were derived in the framework of this model [1,2,5,6,9]. We consider the results of these works in Sect. 4.

1.2. High-velocity penetration (armor piercing) problems

Voluminous literature is devoted to problems of impact interaction between deformed solids. The heightened interest in the high velocity interaction of deformed solids has been stimulated both by fundamental problems of the physics of high pressure, the synergetics of deformed media and material science, and by the expanding range of applied problems that can be solved with the use of axisymmetric and elongated cumulative charges. Because of this, high velocity impact and penetration were traditional subjects in Russian technical literature on mechanics and physics for many years. The term "high-velocity penetration" denotes a dynamic process in which the penetration velocity of a projectile (the displacement velocity for the projectile-target interface) is higher than the velocity of defect propagation [4–6,30–33].

Significant advancement has been observed in these studies beginning in the 1940's and 1950's (see, for example, Refs. [5,32–38]). The development of apparatus and methods for investigating rapidly occurring processes, and the appearance of laboratory ballistics devices have contributed to an improvement in the effectiveness of experimental investigations. The theoretical approach has evolved both due to a more precise definition of the physical nature of the phenomena under consideration, an as result of refinement of computational methods of computer mechanics, and the development of personal computers. Some recent papers in this field are cited in the list of references of the present review (see Refs. [32,33,39–52]).

The classic hydrodynamic theory of high velocity rods striking solids is based on an incompressible inviscid flow model (see Refs. [34–38]). According to this model, the kinetic energy of the projectile goes entirely to the kinetic energy of the target and the projectile's material flow. The hydrodynamic approach implies that the work of plastic deformation and increase in internal energy are negligible as compared to the kinetic energy of the flow. The penetration parameters are determined by the pressure in stagnation point K (see Fig. 1):

$$P_{K_0} = \frac{\rho_0 u^2}{2}, \tag{3}$$

where ρ_0 is the target density and u is the penetration velocity, *i.e.*, velocity of the contact surface (the zero subscript refers to the uncompressed target material). It follows that the resistance of the target to the penetration is determined by the inertial forces. The relation for penetration velocity is given by the Bernoulli equation which equates the pressure P_{K_0}

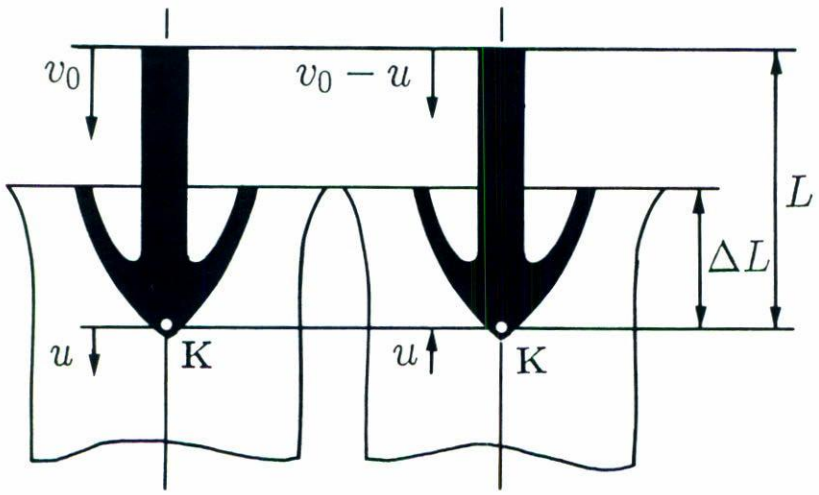

FIGURE 1. Schematic representation of penetration process as an incompressible flow: in the rest coordinate system (a) and in the coordinate system attached to the point, K, of branching of fluxes (b).

at the points where the flows branch to either side of the surface of contact of the rod (the length of which is much larger than its diameter) and the target:

$$P_{K_0} = 0.5\,\rho_0 u^2 = 0.5\,\rho_r (v_0 - u)^2, \tag{4}$$

where v_0 is the impact velocity and ρ_r is the rod density. From Eq. (4) it follows that

$$u = \frac{\lambda v_0}{1+\lambda}, \tag{5}$$

where

$$\lambda = \sqrt{\frac{\rho_r}{\rho_0}}; \tag{6}$$

and at the given density and length of the rod the penetration depth L_0 depends on the target density only:

$$L_0 = \lambda l_0. \tag{7}$$

Because the relations (5), (6) and (7) do not agree with experimental data (see, for example, Refs. [35–43]), some empirical modifications were proposed to the hydrodynamic model, in which the Bernoulli Eq. (4) was augmented by another term, taking into account the stress-related resistance to the penetration of the rod into the target (see, for example, Refs. [5,6,38,40,41,42,43]). The most popular form of such modification is

$$P_{K_0} = \tfrac{1}{2}\rho_0 u^2 + H_t = \tfrac{1}{2}\rho_r (v_0 - u)^2 + H_r. \tag{8}$$

This tactics resulted in the modification of relations (5) and (6) in the form

$$u = \frac{\lambda v_0}{\lambda^2 - 1}\left(\lambda - \sqrt{1 + 2(\lambda^2 - 1)\frac{\Delta H}{\rho_r v_0^2}}\right), \tag{9}$$

where $\Delta H = H_t - H_0$. Correspondingly the penetration depth is given by the equation

$$L_0 = \alpha\lambda l_0, \qquad \alpha = \left(1 + 2\frac{\Delta H}{\rho_0 u^2}\right)^{-1}. \tag{10}$$

Relations (9) and (10) give a good description of the experimental results of Refs. [36–40] with the use of only one adjustable parameter ΔH. However, the lack of any valid justification for the additivity of the strength-related component of the resistance of penetration motivated a search for other modifications of the hydrodynamic model. For example, in Ref. [43] it is proposed a modification of the hydrodynamic model of high velocity penetration of long rods into solid targets that gave the formula

$$u = \frac{\lambda v_0}{1 + \lambda}\sqrt{1 - 2\frac{\Delta H}{\rho_r v_0^2}} \tag{11}$$

a comparison of which with formula (9) shows that for both cases the rod ceases to penetrate the target at the same critical velocity,

$$v_{cr} = \sqrt{2\frac{\Delta H}{\rho_r}}, \tag{12}$$

but the way in which the strength influences the penetration is described differently. Specifically, if the same value of ΔH is used (ordinarily the strength of the rod is ignored, and it is assumed that $\Delta H = H_t$ is the dynamic hardness of the target, equal to

$$H_t = \frac{3(1 - 2\nu)}{1 - \nu} P_{HEL}, \tag{13}$$

where P_{HEL} is the Hugoniot elastic limit, and ν is Poisson's ratio), then according to Eq. (9) the reduction in the velocity of penetration below that of formula (4) begins at somewhat higher velocities v_0 than according to Eq. (11). That is, with model (11) the strength mechanism is "turned on" more abruptly. Attempts to determine why the Eq. (11) is better by comparing calculations with experiments of the existing accuracy in controlling v_0 and determining u cannot, in our opinion, be considered successful, since by varying within adjustable parameter, one can produce directly contradictory conclusions as to which is better, (9) or (11). There also exist many other modifications of the hydrodynamic model of high velocity of penetration of long rod into solid target, whose results can be approximated by the relation of the form

$$L_0 = \kappa\lambda l_0(1 \pm \gamma P^*)^b, \tag{14}$$

where κ is a constant coefficient that characterizes the momentum transfer from the rod to the target, while for the quantities in the parentheses, γ and b are constants of the material and P^* is a function of impact velocity, v_0, which takes into account the effect of the strength (usually, $P^* = \Delta H/\rho_r u^2$). Therefore, according to Ref. [38], even when the target and the rod are made of the same material, ($\lambda = \kappa = b = 1$), H_t and H_r do not coincide, but $2.5 < H_t/H_r < 3$ and $\gamma P^* = -\Delta H/\rho_r v_0^2$, where $\Delta H = 0.66\, H_t$. A more correct way of taking into account the geometric factor, developed in our work [44], showed that with small corrections for the strength of the target ($H_t/\rho_r v_0^2 \ll 1$), and of the cumulative knife ($H_r/\rho_r v_0^2 \ll 1$) the following relations hold in the first approximation:

$$H_t = \frac{H_t^D}{\sqrt{3}} \left[3 \ln \left(2\sqrt{3} \frac{G_t}{H_t^D} \right) - \ln 2 \right], \tag{15}$$

$$H_r = \frac{H_r^D}{\sqrt{3}} \left[1 + \ln \left(\sqrt{3} \frac{G_r}{4H_r^D} \right) \right], \tag{16}$$

where H_t^D and H_r^D are the dynamic yield points of the materials of the target and the plane cumulative knife, and G_t and G_r are their shear moduli. For the case of the penetration of an axisymmetric rod into a semi-infinite target:

$$\Delta H = H_t^D \left[\frac{2}{3} + \ln \left(\frac{3G}{2H_t^D} \right) \right]. \tag{17}$$

The theory of high velocity penetration of porous targets was developed in our works [51,52]. It was shown that the predictions of this theory are in a good agreement with results of experimental investigations [34,42,53].

The method for determination of the parameters which governs processes of high velocity penetration on the basis of quantum statistical models of irreversible deformed solids was proposed in our works [1,5,24,25]. The most important results of these works are considered in Sect. 5 of the present review.

2. QUANTUM-FRACTURE-MECHANICAL MODELS OF DEFORMED SOLID

The usual approach to constructing the quantum fracture mechanics of irreversible deformed solid is based on the use of an interatomic pair wise potential $U(r)$ (see, for example, Refs. [1,7,8,15]) which, independently of the type of interatomic force, has the shape shown in Fig. 2 and characterized by:

1) Minimum in $U(r_{ij})$, which corresponds to the equilibrium interatomic distance r_{ij} at zero absolute temperature ($T = 0$ K) and is determined by the competition of the forces of attraction and repulsion.

2) Position r_m at which the force of interatomic interaction (proportional to $(\partial U/\partial r)$) reach a maximum, *i.e.*, $\partial^2 U/\partial r^2|_{r_m} = 0$.

3) Energy spectrum of this potential represents a set of energy levels, ε_n; in the ground state, an atom, owing to zero oscillations, possesses a finite energy

$$\varepsilon_0 = \frac{\pi\hbar}{r_{ij}}\frac{\sqrt{U(r_{ij})}}{m}, \tag{18}$$

reckoned from $U(r_{ij}) = 0$. Here $\hbar = 1.05 \times 10^{-34}$ J $\times$ s is the Planck's constant and m is the mass of an atom.

4) The amplitude of the *zero atomic oscillations* is equal to

$$\langle \Delta r \rangle = \frac{r_{ij} m C_{\mathrm{a}}}{\sqrt{mU(r_{ij})}}, \tag{19}$$

where

$$C_{\mathrm{a}} = \frac{\pi\hbar}{m r_{ij}} \tag{20}$$

is the *maximum velocity of a finite motion* of atoms in the potential well $U(r)$ at this energy level, and

$$\Lambda_{\mathrm{B}} = \frac{\langle \Delta r \rangle}{r_{ij}} = \frac{m C_{\mathrm{a}}}{\sqrt{mU(r_{ij})}}, \tag{21}$$

is the *De Boer's parameter* (for solids $\Lambda_{\mathrm{B}} \ll 1$ and for quantum crystals $\Lambda_{\mathrm{B}} \sim 1$ [54]).

5) Because of the *Heisenberg's uncertainty principle*, the energy levels of the atoms in the pairwise potential have a finite width. It is easy to show that the energy width of the ground level is equal to

$$\delta\varepsilon_0 = \frac{\pi^2\hbar^2}{2mr_{ij}}. \tag{22}$$

We note that $\delta\varepsilon_0$ is equal to the kinetic energy of an atom for which the *de Broglie wavelength* λ_{D} is equal to interatomic distance, *i.e.*,

$$\lambda_{\mathrm{D}} = 2r_{ij}.$$

This equality corresponds to the velocity of atomic motion $u = C_{\mathrm{a}}$ of the atom.

6) Because of the asymmetrical shape of the potential, $U(r)$, the degeneracy of the levels $n = 1, 2, \ldots$, is lifted. So that the difference in the energies of the neighboring levels, $\Delta\varepsilon_n = \varepsilon_{n+1} - \varepsilon_n$ decreases with growing n. Each energy level is characterized by its stable atomic configuration and specific interatomic spacing, $r_{ij}^{(n)}$. As a rule,

$$r_{ij}^{(n+1)} > r_{ij}^{(n)}.$$

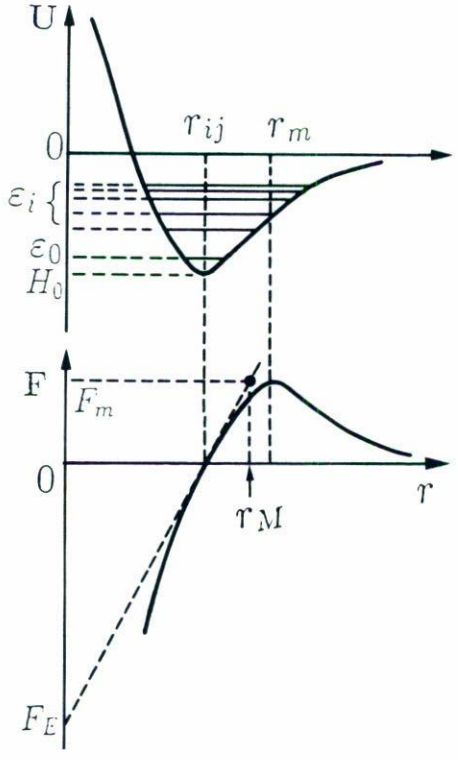

FIGURE 2. The shape of an interatomic pair wise potential and energy spectrum on it.

This condition determines the thermal expansion of a solid.

7) In this analysis, the state of a *quantum crystal* is realized if

$$\Delta\varepsilon_0 < \delta\varepsilon_0. \tag{23}$$

It is well known that under certain conditions helium changes into a quantum-crystal state. The physics of quantum crystals is described, for example in Refs. [54–56].

Using quantum fracture mechanics to solve a problem of the initiation of cracks and dislocations makes it possible to predict the brittle-plastic nature of a specific crystal [9,13]. The difficulties encountered in experimental and theoretical investigations of the dynamic behavior of dislocations are due to the great variety of factors influencing their mobility. Under a given external load the deformation conditions depend on the type of a crystal, the crystal structure of the lattice, the nature of the moving dislocation, and on numerous mechanisms of the interaction related both with the microstructure of the stress field (determined by the characteristics of the real material and by the lattice defects) as well as with various quasiparticle excitations. In discussing this problem it is usual to separate the main dislocation drag mechanisms into two groups. The first group deals with the effect of barriers created at a local obstacle such as impurities, point defects, other dislocations, radiation damage, etc., or by the Peierls potential relief, which is an

unavoidable concomitant of the periodic structure of the lattice. As is well known, such barriers are overcome by thermal or quantum fluctuations. The second group comprises dynamic dissipative processes of the interaction between dislocations and elementary excitations in a crystal, primarily phonons and electrons. This type of interaction is viscous and at low dislocation velocities the drag force is a linear function of the velocity, the coefficient of proportionality representing the viscosity of the quasiparticle gas.

The shortcomings of the quantum theory of solid state and quantum fracture mechanics are associated with the use of interatomic pairwise potential. Actually, however, the states of condensed matter, namely *crystalline*, *amorphous*, *quasicrystalline*, and *liquid* are characterized by strong correlation in the relative positions of atoms at distance, L_0, much greater than $r_{ij}^{(n)}$. In various states of condensed matter the energy of a volume element of the system is a function of the relative arrangement of the atoms. At a given density, the difference between the energies of different local configurations of atoms is large in comparison with the characteristic thermal energy; *i.e.*, the relative positions of the atoms are correlated in a mesoscopic element of the system, which implies the shear stiffness or resistance of a condensed system (including the local shear stiffness of viscous liquids). In condensed matter, only certain configurations of particles occur with an appreciable probability, implying that a definite local structure exist. In a crystal at a sufficiently low temperature the relative positions of atoms are determined to within small fluctuations by the elementary translation vectors of the ideal lattice. The local structure satisfies the conditions of the Fedorov's theorem. At higher temperatures, where the displacement amplitudes of atoms from their local-equilibrium positions become significant, the concept of local structure may be defined [57] and we can treat the instantaneous arrangements of atoms in an element of the condensed matter as a result of displacements from certain ideal positions. Therefore, the rheological behavior of real deformed media is governed by the dynamics of collective excitations. This fact has also predetermined the successful use of the ideas and methods of *synergetics* in solid mechanics (see, for example, Refs. [1,22,47,58–60]).

3. QUANTUM-STATISTICAL FRACTURE MODEL OF DEFORMED SOLID

The spectrum of *structural excitations* (defects) in deformed solids can be determined correctly from the solution of the non-steady-state equations of *stochastic mechanics* (see Refs. [1,2,61]) with the potential $V_{ij}(r)$ that is formed by an ensemble of atoms. This potential determines the "structural memory" of the deformed solid. Analytical solution of the equations of stochastic mechanics in the general case is, obviously, impossible. However, the main properties of the collective motion of excitated atoms can be established prior to the complete solution of these equations. Probably, it would be sufficient to use the approximation of the potential relief V_{ij} in the following general form:

$$V_{ij}(r) = V_{ij}^0 f(r), \tag{24}$$

where $f(r)$ is a periodic (quasiperiodic) function with period $2a_0$ that is defined on the

scale of the order of $\sim L_0$, and

$$V_{ij} = \begin{cases} U(r), & |r_i - r_j| \leq a_0, \\ V_0 |r_i - r_j|^{-\alpha}, & |r_i - r_j| > a_0. \end{cases} \tag{25}$$

Here $U(r)$ is a V–shaped potential which is defined by interatomic interaction within the first coordination sphere of radius a_0; this determines the compressibility of the solid, which is characterized by the *bulk modulus* B, as

$$B \propto \oint_{a_0^3} U(r)\, d^3 r,$$

while $V_0 |r_i - r_j|^{-\alpha}$ takes into account the long-range interatomic correlation, which determines the shear stiffness of solid, characterized by the shear modulus $G = \rho C_t^2$, where ρ is the density of the matter and C_t is the velocity of transverse acoustic waves (in a liquid $C_t = \nu / L_0$, where ν is the dynamic viscosity and L_0 is the characteristic length of energy dissipation).

The following properties can be shown in this general case:

1. Because two atoms cannot located in the same site of the potential relief which is formed by the system of atoms, the lattice sites closing follows the Fermi statistics. In most crystals the thermal movement of the atoms at temperatures considerably below the melting point has the character of small vibrations about the crystal lattice nodes. The smallness of the vibrations implies that the mean thermal displacement of an atom from the node is very small in comparison with the lattice constant a_0, *i.e.*, $\langle \Delta r \rangle \ll a_0$. In this case

$$\Lambda_B \ll 1, \tag{26}$$

and in an ideal crystal at the temperature $T = 0$ K, all the atoms are in the lowest energy level (ground state)

$$\varepsilon_0 \simeq \tfrac{9}{8} K_B \Theta_D, \tag{27}$$

where $K_B = 1.380662 \times 10^{-23}$ J/K is Boltzmann's constant and Θ_D is the Debye temperature of a solid.

The width of the ground energy level is defined by Eq. (5). It is necessary to note that even in the case $\Lambda_B \ll 1$ the energy of the zero-point oscillations is not small. If the temperature of a solid

$$T < \tfrac{2}{3} \Theta_D, \tag{28}$$

then the energy of zero-point oscillations is higher than energy of thermal oscillations. For the majority of materials ε_0 has the order $0.2\, H_m$, where H_m is the melting energy,

and approximates to the energy of structural transformation if it exist. For example, for titanium:

$$\varepsilon_0/H_{\mathrm{m}} = 0.29, \quad \varepsilon_0/H_{\alpha\to\beta} = 0.71;$$

and for zirconium:

$$\varepsilon_0/H_{\mathrm{m}} = 0.20, \quad \varepsilon_0/H_{\alpha\to\beta} = 0.71.$$

Here $H_{\alpha\to\beta}$ is the energy of $\alpha \to \beta$ phase transition from hexagonal structure to body centered cubic structure [2].

2. For quantum crystals, such as helium quantum crystal, the magnitude of zero-point oscillations (see Eq. (19)) is comparable with the interatomic distance r_{ij} and

$$\Lambda_{\mathrm{B}} \sim 1. \tag{29}$$

For example, ^{3}He has $\Lambda_{\mathrm{B}} = 0.49$, ^{4}He has $\Lambda_{\mathrm{B}} = 0.43$, H_2 has $\Lambda_{\mathrm{B}} = 0.28$, and Ne has $\Lambda_{\mathrm{B}} \approx 0.1$. There are other example for which $\Lambda_{\mathrm{B}} \geq 1$ (see Refs. [54–56]). This refers to admixtures of light elements in matrices of heavy metals. Owing to their small mass and weak interaction with the atoms of the matrix, the atoms of the impurity are characterized by a parameter $\Lambda_{\mathrm{B}} \geq 1$. For example, this happens for hydrogen in matrices of niobium, zirconium, palladium, etc.

In all these cases the fundamental assumption of solid state quantum theory that particles and crystal nodes correspond, breaks down. Because of this, any defects in quantum crystal are delocalized and all atoms of quantum crystal are in the state of zero-motion, that is accompanied by transfer of the atoms between sites of crystal lattice therewith the number of atoms is not equal to the number of sites in crystal lattice. On the other hand, the particles forming the crystal are generally identical. In quantum mechanics identical particles are indistinguishable. A situation arises in which a multitude of identical particles exists in a discrete crystal lattice, the wave functions of which overlap strongly owing to the large magnitudes of amplitudes of the zero-point vibrations. The overlap of the wave functions implies that the atoms are actually converted into moving quasiparticles in the space of the crystal lattice. One can no longer say that each particle corresponds to one definite lattice node. Any atoms can exist at any node.

Evidently, two particles cannot exist simultaneously at the same lattice node. Therefore an infinitely large repulsion exists when the coordinates of two quasiparticles coincide. This is described by an "impenetrability" potential of quasiparticles at the same lattice node. Therefore it is important to take into account the correlation between particles as they approach one another.

Thus numerous crystals exist that clearly manifest the following features:

a) the energy of the ground state of the crystal is altered by the presence of a large repulsion between the quasiparticles;

b) the atoms are converted into moving quasiparticles in lattice space;

c) the wave functions of the atoms overlap, leading to a finite probability of tunneling of atoms from one node to another, and as a result, the *quasiparticle* ("*vacancion*") *band* is formed as the analog of the conductivity band for electrons in metals (see, for example Refs. [54]).

At non-zero temperature the crystal tends to have a minimal free energy. Hence it can lose a little energy while slightly increasing in disorder. The conflict between this is minimal when a certain number of vacancies exists —nodes not containing atoms. Owing to the large amplitudes of zero-point vibrations of the atoms, these vacancies become vacancions— quasiparticles characterized by a certain value of the energy ε and quasimomentum $\vec{p}$. Thus, a quantum crystal contains a gas of vacancions* whose displacements are equivalent to the displacement of atoms.

Vacancions can exist even at absolute zero temperature: zero-point vacancions. In this case they also can move in the crystal in the equilibrium state. One can picture a quantum crystal as though it contained within itself a liquid consisting of zero-point vacancions, and hence capable of moving easily through the crystal lattice. The flow of this liquid is accompanied by transport of matter. In contrast to an ordinary liquid, here the direction of mass transport opposes the direction of flow of the vacancion liquid. The vacancions lower the energy of the ground state of the crystal [56]. The bottom of the vacancion band lies below the energy of the ground state of the crystal. Energy width of the vacancione band is proportional to the quantum tunneling frequency $(\tau_{ij}^{\mathrm{T}})^{-1}$ of atoms in crystal lattice:

$$\Delta \propto (\tau_{ij}^{\mathrm{T}})^{-1} \propto \frac{J}{\hbar}, \tag{30}$$

where J is the jump integral which governs the momentum of quasiparticles in a quantum crystal:

$$p = \hbar m a_0 J. \tag{31}$$

In a certain sense, quantum crystals having zero-point vacancions are analogous to metals, *i.e.*, crystals containing a liquid consisting of electrons. The electron liquid in a metal also can move easily through the crystal lattice. But every change in the electron density is accompanied by appearance of charge density, which gives rise to very strong electric fields, owing to which the spatial redistribution of mass of the material does not occur. In a metal a vacancy is an electrically neutral object.† The flow of the vacancion liquid in a quantum crystal can be accompanied by a change in the spatial distribution of matter.

Quantum crystals are strongly anharmonic even at absolute zero and therefore possess unique properties, in particular, an essentially new motion of the atoms is possible in them: quantum diffusion (see Refs. [1,2,54–56]).

---

*It is more properly to use the term "vacancion liquid" because the motion of vacancions has more direct analogy with liquid flow (there is not the charge of volume).

†In ionic crystal a vacancy has electrical charge (see, for example, Ref. [62]) and by this reason the discussed phenomenon of mass transfer by vacancions flow in ionic crystals is more complex.

Any defects in crystals in which the parameter Λ_B is not a small quantity in comparison with unity are delocalized and become quasiparticles —defectons, which are characterized by a certain value of the energy and quasimomentum.

A light impurity atom in a quantum crystal also behaves like a quasiparticle —an impuriton or *mass-fluctuation wave* [54].

A quantum crystal is a highly specific state of matter. As we have noted above, its density distribution is periodic in space. That is, in symmetry it resembles an ordinary crystal, but in the character of motion of quasiparticles it occupies a position intermediate between a liquid and a solid. A first form of motion has the property of motion in a liquid —this is the flow of the vacancion liquid with immobile lattice nodes. In a gravitational field a quantum crystal can flow from vessel to vessel analogously to liquids. However, the flow here is peculiar: the transfer of matter from top to bottom is effected by flow of the vacancion liquid from bottom to top over the crystal lattice nodes. The motion of the above stated quasiparticles is a quantum diffusion in lattice space, which has been found experimentally in Khar'kov, Russia (Grigor'ev, Esel'son, Mikheev, Shul'man) and in Sussex, England (Richards, Pope, Windom) in 1977. The diffusion coefficient is an important, experimentally measurable characteristic of the gas of quasiparticles (see Ref. [56]).

Depending on the statistics of the original atoms comprising the crystal, the quasiparticles in a quantum crystal obey either Bose-Einstein or Fermi-Dirac statistics. Both of these excitations can be found in a crystal in different concentrations or in the form of a solution of Fermi-Bose quasiparticles. A striking example of a quantum crystal is the ^{3}He–^{4}He solution. Phenomenological equations of hydrodynamics describing the macroscopic motions in quantum crystals have been proposed by Andreev and Lifshitz (see Ref. [63]).

3. It is apparent that for crystals with defects there is discordance between the number N_a of atoms and the number N_0 of potential sites on a lattice. As indicated below, if concentration of defects has more than the critical value, this discordance gives rise for delocalization of defects in crystal lattice even in the case $\Lambda \ll 1$.

If the ratio

$$n = \frac{N_a}{N_0} < 1, \tag{32}$$

then the *Hamiltonian* of the system can be written in the form of the *Hubbard Hamiltonian* [64]

$$H = \sum_{ij} U_{ij}\, d_i^+\, d_j. \tag{33}$$

Here U_{ij} describes the transition of an atom localized at a site j to its nearest neighbor i; and

$$d_i^+ = (1 + a_i^+ a_i) a_i^+, \tag{34}$$

where a_i^+, a_i are the atom operators.

Equation (33) yields the following expression for the average energy:

$$\langle H\rangle = \sum_k U(\vec{k})\langle d_i^+ d_j\rangle_{\vec{k}}, \tag{35}$$

where $U(\vec{k})$ and $\langle d_i^+ d_j\rangle_{\vec{k}}$ are the components of the *Fourier transform* of U_{ij} and $\langle d_i^+ d_j\rangle$, respectively, Here,

$$\langle d_i^+ d_j\rangle_{\vec{k}} = \int R_k(\varepsilon)\, d\varepsilon \tag{36}$$

(see Ref. [65]), where

$$R_k(\varepsilon) = \left[1 + \exp\left(\frac{\varepsilon - \mu}{K_B T}\right)\right]^{-1} \left(\langle\langle d_i/d_j^+\rangle\rangle_{k,\varepsilon+iE} - \langle\langle d_i\rangle\rangle_{k,\varepsilon_i E}\right)\Big|_{E\to 0}, \tag{37}$$

μ is the chemical potential, and $\langle\langle d_i/d_j^+\rangle\rangle_{k,\varepsilon}$ are the components of the Fourier transform of the Green's functions, $\langle\langle d_i/d_j^+\rangle\rangle$. These Green's functions are given by the equation

$$\varepsilon\langle\langle d_i/d_j^+\rangle\rangle = \frac{\delta_{ij}}{2\pi}(1-n) + \langle\langle [d_i H]_-/d_j^+\rangle\rangle_\varepsilon. \tag{38}$$

We shall set

$$\langle\langle [d_i H]_-/d_j^+\rangle\rangle_\varepsilon = A\sum_t U_{it}\langle\langle d_t/d^+ j\rangle\rangle_\varepsilon + B\langle\langle d_i/d_j^+\rangle\rangle_\varepsilon. \tag{39}$$

In our case, the actual form of the coefficients A and B is irrelevant. As a result, we obtain

$$\langle\langle d_i/d_i^+\rangle\rangle_{k,\varepsilon} = \frac{1-n}{2\pi(\varepsilon - \varepsilon(k))}, \tag{40}$$

and

$$R_k(\varepsilon) = \frac{(1-n)\delta(\varepsilon - \varepsilon(k))}{1 + \exp[(\varepsilon - \varepsilon(\vec{\varepsilon}))/K_B T]}. \tag{41}$$

The ground-state energy is given by equation

$$\varepsilon_0 = \frac{1}{N}\sum_k (1-n)U(k)\,\Theta[\mu - \varepsilon(\vec{k})], \tag{42}$$

where

$$\Theta = \begin{cases} 1, & x > 0, \\ 0, & x < 0. \end{cases} \tag{43}$$

Using the approximation of the density of the atom states in the form

$$\begin{cases} \dfrac{1}{N}\sum\limits_{k}\delta[\varepsilon - U(k)] = U_0^{-1}, & |\varepsilon| \le 0.5\,U_0, \\ 0, & |\varepsilon| > 0.5\,U_0, \end{cases} \tag{44}$$

we obtain the expression for the ground-state energy

$$\varepsilon_0 = 0.5\,U_0\,n(1-n). \tag{45}$$

We can write Hamiltonian (33) in the following form:

$$H = \sum U_{ij}^{\mathrm{e}}\, a_i^{+}\, a_j, \tag{46}$$

where U_{ij}^{e} is effective transfer integral. From Eqs. (35) and (46) it follows that

$$U_{ij}^{\mathrm{e}} = \frac{4(1-n)}{(2-n)^2}\,U_{ij}. \tag{47}$$

That is the increase of the concentration of defects must occur with an increase of effective transfer integral. As a result, if

$$n < n_{\mathrm{cr}}, \tag{48}$$

then

$$U_{ij}^{\mathrm{e}} > U_0 = mC_{\mathrm{a}}C_{\mathrm{t}} = mC_{\mathrm{S}}^2, \tag{49}$$

and atoms of a solid are delocalized. This is reflected in the fact that vacancione band in solid is formed as a analog of the vacancione band in quantum crystal. By this means mass transport in solid with defects can be accounted for in two ways:

a) as a result of the motion of atoms, accompanied by the displacement of the sites of crystal lattice,

b) as a result of an atom stream on fixed sites of lattice (analogous to the liquid flow). The parameter

$$C_{\mathrm{S}} = \sqrt{C_{\mathrm{a}}C_{\mathrm{t}}} \tag{50}$$

is the *stability of crystal lattice mass velocity.* As we shall show below, if the momentum of atoms in crystal lattice $p > mC_{\mathrm{S}}$ then these atoms are delocalized. This means that crystal lattice loses its stability and a crystal goes over to the non-equilibrium state.

Notice that for a crystal that satisfies condition (26) under standard quasistatic loading, condition (32) is beyond reach, since the crystal disintegrates at a smaller concentration of defects. But already in the classic work of Bridgman [66] it was established that under the simultaneous action of hydrostatic and shear stress diffusion processes intensify to an extreme extent and solid flow like as liquid, while remaining in a crystalline state.

4. The effect of interatomic action at a distance results in a power dependence of the correlation function of atoms in condensed matter [63],

$$\langle n(a)\, n(a-r)\rangle \sim r^{-\alpha}, \tag{51}$$

which is characteristic of *fractal structures* (see, for example, Refs. [1,12,67]). The exponent in Eq. (51) is determined by the *fractal dimension* D_{F} of the wave functions ψ_i of the atoms formed the solid and the *topological dimension* d *of the Euclidean space* [1,21,67]:

$$\alpha = d - D_{\mathrm{F}}. \tag{52}$$

As a result the *structural excitations* in crystal can be either irrotational ($\operatorname{curl}\vec{u} = 0$), for example vacancies, interstitial atoms, edge dislocations, etc. or solenoidal ($\operatorname{div}\vec{u} = 0$), for example screw dislocations and disclinations; the latter type also caused significant rotational modes of deformation, studied, for example in [68]. However, only a restricted set of atomic configurations can be realized with a significant probability in the elements of a condensed matter having volume of the order of $\sim L_0^3$, where L_0 is the mean length of relaxation of momentum of atoms in crystal lattice [1].

Because of this, in order to determine D_{F} for Eq. (52) the discussion may be shifted from the atomic level to the mesoscopic level, where the exponent α can be expressed in terms of *Poisson's ratio* ν, which specifies the change in volume during longitudinal deformation of a solid:

$$\alpha = 1 - 2\nu. \tag{53}$$

Hence, using Eqs. (52) and (53) and bearing in mind that $d = 3$, we obtain the relationship for fractal (metric) dimension of the wave functions of atoms in the form

$$D_{\mathrm{F}} = 2(1+\nu). \tag{54}$$

Since $0 < \nu < 0.5$, where the lower and upper limits are a consequence of the *Le Chatelier-Brown principle of stability* for elastic lattice, we have $2 < D_{\mathrm{F}} < 3$.

5. Typical energy spectrum of atom excitations in a crystal lattice is shown in Fig. 3a. When $T > 0$ K, some of the atoms enter higher energy states corresponding to different kinds of quasiparticle (vacancies, interstitial atoms) and collective structural excitations (dislocations, disclinations, etc.). These transitions are accompanied by the emission and absorption of the *collective Bose excitations* (density and shape fluctuations) with dispersion curves of the type shown in Fig. 3b. The interaction of the excitations causes a

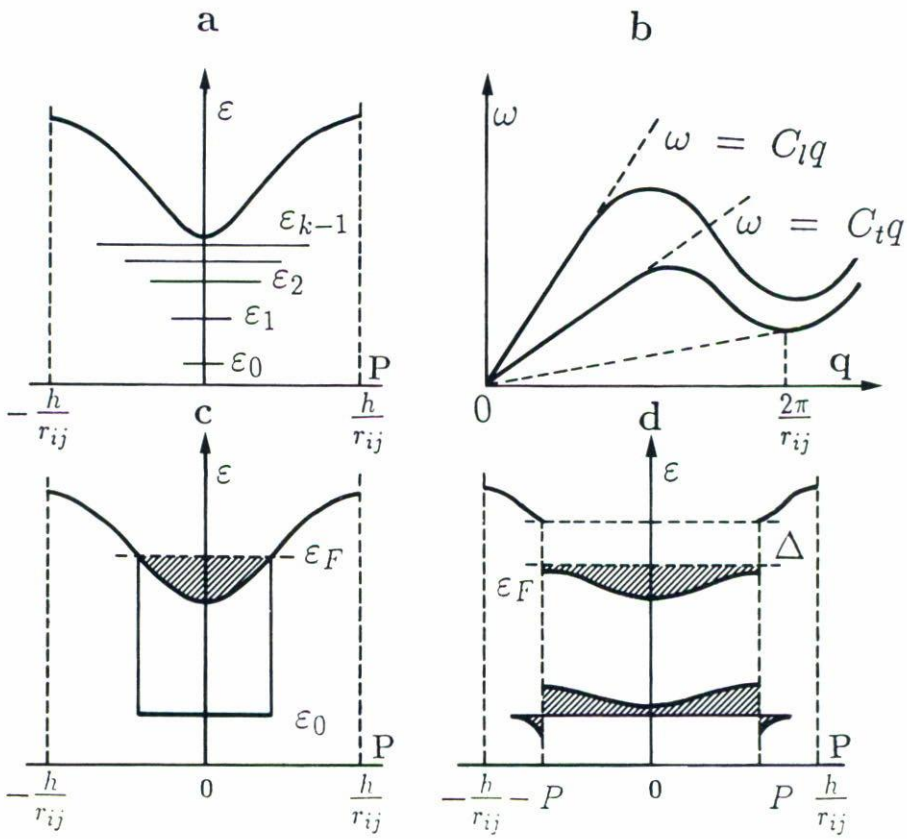

FIGURE 3. The energy spectrum of atoms in a crystal with defects and changes in the spectrum as a result of kinetic phase transitions at the critical values of the momentum of atoms (these changes cause changes in the behavior patterns of dynamic deformation of a solid) [25]: (a) in a state of thermodynamic equilibrium, (c) for $mC_S < p < mC_{cr}$, (d) for $mC_{cr} > p > mC_l$; and a spectrum of Bose-type excitations in crystal with defects (b).

splitting of the energy levels which is responsible for the formation of the *mobility bands* (these bands are the analogs of vacancion bands in quantum crystals and also analogs of the *conductivity bands* of electrons in semiconductors and dielectrics).

6. The wave function ψ, of atoms in crystal satisfies the Schrödinger equation

$$\frac{\hbar^2}{2m}\Delta\psi_i + \varepsilon\psi_i = -\sum_j V_{ij}\,\psi_i, \tag{55}$$

with the potential governed by Eqs. (24),(25). When short- and long-range interactions exist, spatial dependence of the wave function is characterized by a *hierarchy of lengthscales*, which obviously determine the spatial scales of the *structural levels* of plastic deformation and fracture of solids (see Refs. [1,2,21]).

TABLE I. Parameters of quantum-statistic model for some materials [25].

	Material						
	Cu	Ag	Au	Al	Diamond	Si	Glass
C_a, m/c (3)	13	6.4	3.5	26	109	30.4	44
Re_{cr}	0.93	0.85	1.01	1.14	0.54	0.52	0.58
L_0	0.9	1.6	2.1	0.7	0.35	0.85	—
$(\sigma_{cv}/G) \times 10^5$	2.6	1.3	0.8	6.4	7.8	1.2	11.5

7. The relaxation time $\tau_p^{(n)}$ of a momentum of atoms ($n = 0$) and of structural excitations of the n–th level is much less than the time of energy relaxation, *i.e.*,

$$\tau_\varepsilon^{(n)} \gg \tau_p^{(n)},$$

where

$$\tau_p^{(0)} \sim \frac{a_0}{\sqrt{C_a C_t}} = \frac{L_0}{C_t}, \qquad \tau_\varepsilon^{(0)} \sim \frac{a_0}{C_a}. \tag{56}$$

Here L_0 is the mean length of relaxation of momentum of atoms in crystal lattice and C_S is defined by Eq. (50). By this means

$$L_0/a_0 \sim \sqrt{C_t/C_a} \gg 1.$$

For this reason, localized far-from-equilibrium regions are formed in deformed solid even under comparatively small loads,

$$\sigma \sim \sigma_{cv} = 0.5\rho C_a^2. \tag{57}$$

It can be seen from Table I that $\sigma_{cv} \sim 10^{-5}G \sim 1$ MPa (where $G = \rho C_t^2$ is the shear modulus), in agreement with experimental data (see Ref [69]).

8. An external influence causes a redistribution of the atoms among the energy states if the stress obeys $\sigma > \sigma_{cv}$, where σ_{cr} is defined by Eq. (57). When $\sigma > \sigma_{cv}$, the response of a deformed solid is determined by the superposition of structural (s) and condensate (c) components associated with mixing of defects in the stress field and with forced Bose-condensation of induced density and shear fluctuations (analogous to the forced Bose-condensation of photon in laser). For example, plastic deformation is given by the expression

$$\epsilon_p = \epsilon_c + \epsilon_s(t),$$

which is in accordance with the scheme whereby experimentalists (see, for example Refs. [70,71]) separate $\epsilon_p(t)$ into sudden and time-dependent components. Thus, structural

(for example, dislocation), condensation (dilation [72]), and mixed mechanisms for crack formation may be realized.

9. If the stress σ applied to a solid exceeds a critical value σ_{cv}, irreversible creep occurs, manifested by a steady increase in the plastic strain ϵ_p with time t under a constant stress and by incomplete relaxation of $\epsilon(t)$ to the initial value $\epsilon(0) = 0$ when the load is removed. Depending on the temperature, there can be transient and stress-state creep with, respectively, a very slow (approximately logarithmic) and a linear increase in the strain with time. The first type is observed experimentally at temperatures T less than half the melting point T_m and shows a decrease of the strain rate $\dot{\epsilon} \equiv d\epsilon/dt$ to zero under constant load. The second type is observed for $T > T_C \sim 0.5\,T_m$, and here $\epsilon_p(t)$ for $t \to \infty$ reaches a value $R(\sigma) \neq 0$. Far from the melting point, the dependence of R on the applied stress σ is given by a power law

$$R(\sigma) \propto \sigma^n, \tag{58}$$

with $3 \leq n \leq 4.5$, if σ is well below the theoretical strength $\sigma \ll \sigma_{max} \sim 0.1\,G$; and an exponential

$$R(\sigma) \propto \exp\left(C\frac{\sigma}{T}\right) \tag{59}$$

with $C = \text{const.}$, if $\sigma < \sigma_{max}$. When $T \leq T_m$, diffusion creep is observed, with a linear dependence $R(\sigma)$; this occurs also for small loads σ [70].

10. The free energy in the configurational space of states of a solid under a load $\sigma > \sigma_{cv}$ is shown on Fig. 4a. The fractal dimension of the thermodynamic potential in configurational space of states is $d_F = D_F - 1$. In the approximation of central nearest-neighbor interactions, the Cauchy relations give us $\nu = 0.25$, from which it follows $\alpha = 0.5$, $D_F = 2.5$, $d_F = 1.5$. Detailed form of the free energy in configuration space with a finner resolution of the defect structure and corresponding ultrametric space are shown in the Fig. 4b, c.

11. Spatial distribution of collective excitation in a deformed solid is self-similar. The fractal dimension of inhomogeneous field of such excitations is defined by Eq. (54). There exists a hierarchy of characteristic spatial scales (of collective excitations in a deformed solid ($n = 0, 1, 2, 3, \ldots$)) described by the ratios

$$æ = \frac{L_{n+1}}{L_n} = \frac{\operatorname{curl}\operatorname{curl}\vec{u}}{\operatorname{grad}\operatorname{div}\vec{u}} = \frac{2(1-\nu_e)}{(1-2\nu_e)}, \tag{60}$$

where $\vec{u}$ is the material vector velocity. Such an hierarchy manifests itself in the self-organization of structural levels of deformation and fracture of solids that are not connected with the initial structure of the material (see Refs. [1,2,7,25]). Here ν_e is the effective coefficient of transverse deformation, which equals ν only in the case of elastic deformations. Since the possible values of Poisson's ratio for solids lies in the range

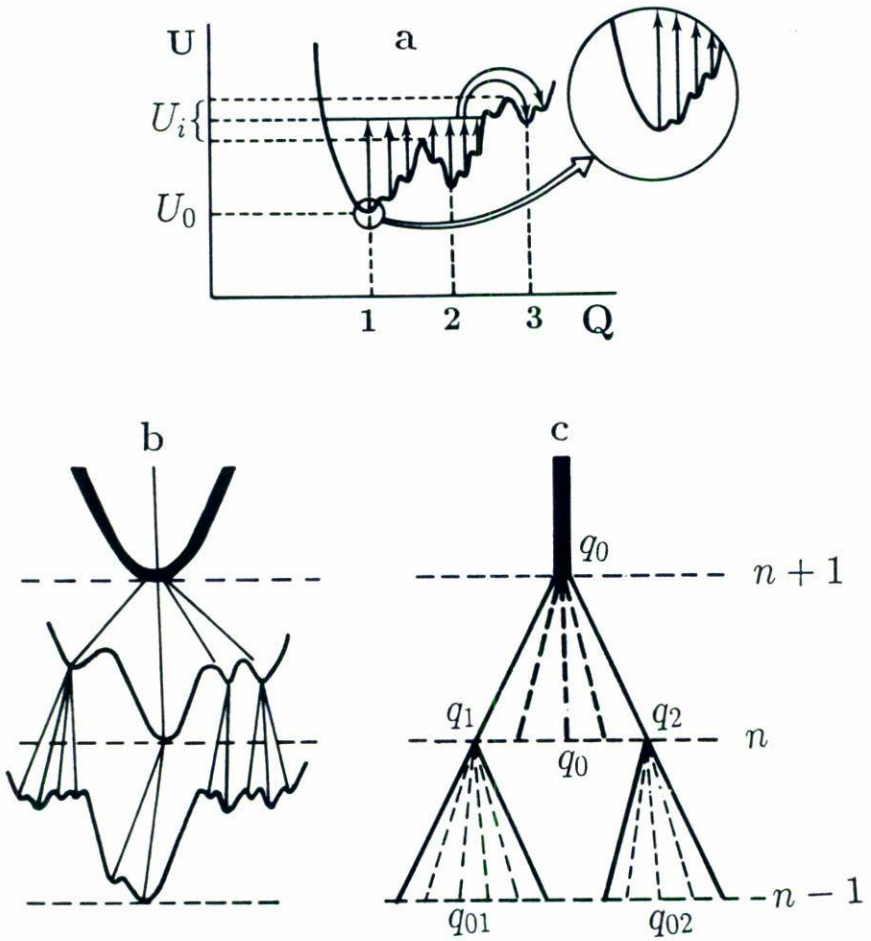

FIGURE 4. Free energy in the configuration space of states of a solid containing defects under a load $\sigma > \sigma_{cv}$ (a); details of the curve of the thermodynamic potential as a function of wave vector (b) and the corresponding ultrametric space (c).

$0.165 \leq \nu \leq 0.475$ [73], æ can vary from 2.5 to 3.0, and the value $\nu = 0.3$, characteristic of most natural materials, corresponds to æ = 3.5, which agrees with the empirically established [21,74] range of variation of relative scales of structural levels of fracture of solids (see Table II), with the most probable value equal to 3.5.

Notice that the Poisson's ratio for metals, alloys, and metal compounds in the elastic region is determined by the structural value, ν_0, and the constant of the electron-phonon coupling, λ, as [2,75-79]

$$\nu = \frac{\nu_0 + \frac{1}{12}(2 - 3\nu_0)\lambda f(T)}{1 - \frac{1}{12}(2 - 3\nu_0)\lambda f(T)}, \tag{61}$$

TABLE II. Particle discreteness in grain-size analysis for rock grinding products [83].

Processing	$L_n \times 10^3$, m	L_{n+1}/L_n
Crusing	228 ± 77	3.1 ± 1.7
	74 ± 16	4.9 ± 2.4
	15 ± 4	3.0 ± 1.4
	5 ± 1	3.3 ± 0.8
	1.5 ± 0.1	4.0 ± 1.5
Powdering	170 ± 14	2.3 ± 0.5
	74 ± 11	2.3 ± 0.4
	32 ± 2	2.7 ± 0.7
	11.7 ± 1.8	3.3 ± 1.2
	3.0 ± 0.7	3.8 ± 0.4

where

$$f(T) = \frac{\int d\vec{p}\,\frac{\partial n}{\partial \varepsilon_{\vec{p}}}}{\int d\vec{p}\,\delta(\varepsilon_{\vec{p}} - E_{\mathrm{F}})}$$

is the function determining the temperature dependence of the effective density of electron states, $f(T = 0) \equiv 1$; n is the Fermi function, $\vec{p}$ is the momentum of electron, $\varepsilon_{\vec{p}}$ is the electron energy spectrum, E_{F} is the Fermi energy, and $\delta(\ldots)$ is the Delta function. For BCC metals and their disordered alloys ν_0 equal to 0.25, and for metal compounds with A 15 structure $\nu_0 = 0.296$ [78,79]. As have been shown in these works, theoretical calculations by Eq. (61) are in an excellent agreement with experiments.

12. The relation (60) characterizes the self-similar regimes of deformation and fracture of solids observed experimentally under certain conditions. However the existence of not less than three independent length scales

$$a_0, \qquad L_0 = a_0 \times \left(\frac{C_{\mathrm{t}}}{C_{\mathrm{a}}}\right)^{1/2}, \qquad L_p = æ L_0,$$

even in elastically isotropic solids, give rise to the complicated dynamics of self-organization of dissipative structures and, in particular, the possibility of formation of incommensurate dissipative structures, having a new set of independent length scales, obtained as a result of dynamic mixing of the starting scales (see Refs. [1,22]). The incommensurate dissipative systems can be formed as a result of the kinetic phase transitions —accompanying a change in the parameters of the perturbation— and as a result of the scale phase transitions (see Refs. [1,47]) —accompanying an increase in the dimensions of the deformed solid body.

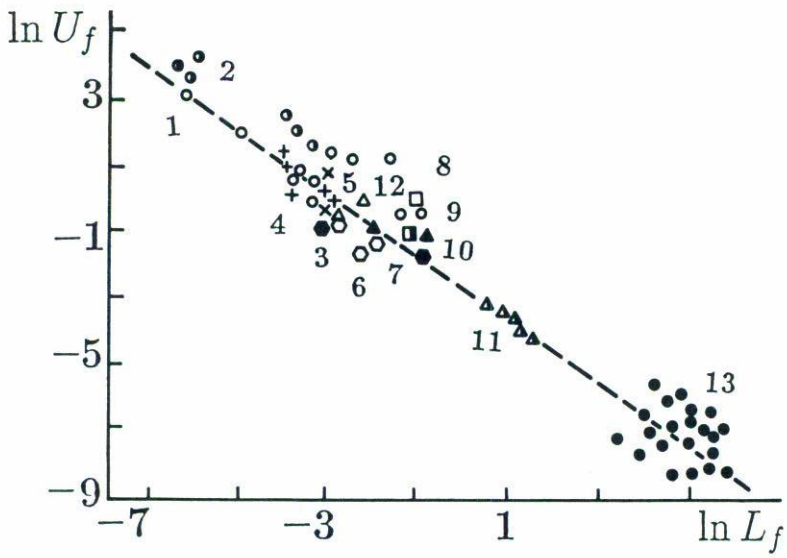

FIGURE 5. The dependence of specific failure energy on size: 1) quartz, 2) glass, 3) marble, 4) clinker, 5) porphyry, 6) coal, 7) gabbro, 8) diabase, 9) drilling, 10) explosion, 11) rock bursts, 12) impact, 25 m/s, 13) earthquakes. The line represents the analytic expression (63) found by least-squares fitting.

13. The limiting value potential energy of elastic strains that can be accumulated in autolocalized structural excitation of the n–th level is proportional to $(L_n)^{D_f^{(n)}}$, where

$$D_f^{(n)} = \frac{2(1-\nu_e^{(n)})}{1-2\nu_e^{(n)}}$$

is the dimension of the structural excitations of the n–th structural level, which is determined by the effective structural value of $\nu_e^{(n)}$. It is easy to see that $D_f^{(n)} > 4/3$. The intensity of entropy export from the far-from-equilibrium regions where an excessive energy is autolocalized (controlling the kinetics of self-organization of dissipative structures), is determined by the fractal dimension of the surface of the far-from-equilibrium regions, $D_F^{(n)} = 2(1+\nu_e^{(n)})$. According to the S-theorem (see Ref. [80]) the self-organization of a dissipative structures in open systems is accompanied by a decrease in the entropy and in entropy rate production, which are normalized to a constant value of the mean kinetic energy. Analog of the S-theorem for processes of self-organization of dissipative structures in a deformed medium may be represented in the form of the D–theorem (see Ref. [24]):

$$D_F^{(n)} < D_F^{(n+1)}, \qquad D_f^{(n)} > D_f^{(n+1)}, \tag{62}$$

from which it follows that limiting energy density is not invariant, since

$$\langle \varepsilon(r)\, \varepsilon(r') \rangle \propto r^{-\alpha_n}. \tag{63}$$

The experimental data for dependence of the specific fracture energy on size of solid are given in Fig. 5. This dependence is in agreement with Eq. (63).

14. The generalized equations of the transport of mass, momentum, and energy (including heat) in a deformed solid can be written in the form

$$\frac{\partial^{\beta}\vec{u}}{\partial t^{\beta}} = D_{\beta}\frac{\partial^{\gamma}\vec{u}}{\partial x^{\gamma}}, \tag{64}$$

where D_{β} is the effective diffusion coefficient (the thermal conductivity, etc.); and $\partial^{\beta}/\partial t^{\beta}$, $\partial^{\gamma}/\partial t^{\gamma}$ are the fractional derivatives with respect to time and coordinate. In homogeneous media β and γ are equal and are determined by the fractal dimension $D_{\mathrm{F}}^{(n)}$:

$$\beta_n = 1 + 2\nu_{\mathrm{e}}^{(n)}; \tag{65}$$

and in materials with multifractal microstructure $\beta/\gamma = \theta$, where $\theta \neq 1/2$ is the exponent of anomalous diffusion, which is defined by equation: $D_{\beta} \propto r^{\theta}$ (see, for example, Ref. [81]).

The use of fractional derivatives permits a simplification of the mathematical form of the transport equations in far-from-equilibrium systems and gives them a graphical interpretation. To elucidate the physical meaning of a transition to a space with a fractional dimension, it is convenient to write Eq. (64) in integral form:

$$G(t) = \int_0^t K(t-\tau)\,u(\tau)\,d\tau, \tag{66}$$

where $K(t-\tau)$ is a memory function (the relaxation kernel, the creep kernel, etc. [18,82]).

In the case of no memory, $K(t-\tau) = \delta(t-\tau)$, the delta function (a Markov's process): $\beta = 2$; *i.e.*, the transport field is not self-similar ($D_{\mathrm{F}} = d = 3$). With complete memory $K(t-\tau)$ is equal to 1 for $\tau < t$ and zero for $\tau > t$; $\beta = 0$, which corresponds to $D_{\mathrm{F}} = 1$. In the general case,

$$K(t-\tau) \sim (t-\tau)^{D_{\mathrm{F}}-1},$$

i.e., the fractal dimension of the transport fields in deformed media is determined by the "memory" of the medium. In this case the invariant is the product

$$D_{\beta_n} \times \varepsilon_{\mathrm{m}}^{(n)} = \text{const.}, \qquad n = 0, 1, 2, \ldots, \tag{67}$$

where $\varepsilon_{\mathrm{m}}^{(n)}$ is the limiting density of energy that can be accumulated in a volume of the order of $\sim L_n^3$. The relation (67) is in agreement with experiment [83].

15. For creep of a solid material it is easy to obtain with the Laplace-Carson transform (see, for example Refs. [82,84]) an expression for D_{F} in the form

$$D_{\mathrm{F}} = \frac{6}{2+\omega}, \qquad \omega = \frac{R(t)}{3B} \leq \frac{2G}{3B}, \tag{68}$$

where B, G and $R(t)$ are the bulk modulus, shear modulus and relaxation modulus. Thus we have

$$1 < \beta = \frac{4-\omega}{2+\omega} \leq 3. \tag{69}$$

This result was used in Refs. [20,82] for developing the theory of plasticity with fractal yield surface.

4. QUANTUM-STATISTICAL MODEL OF DYNAMIC DEFORMATION OF SOLIDS

The relationship between the structural parameters of a material and its dynamic strength is displayed largely under conditions when the influence of defect nucleation and propagation is not decisive in the deformation and fracture of solids. In particular, such conditions are created when the rate of loading is higher than that of defect propagation. From this standpoint, the investigation of the behavior of solids upon high-velocity impact is of interest. Below we consider the response of a solid to shock loading which imparts a momentum $\vec{p} = m\vec{u}$ to the atoms ($\vec{u}$ is a macroscopic mass velocity of the atoms of a solid).

By using considered above quantum-statistical model it is easy to show that if

$$p < mC_{\mathrm{a}}, \tag{70}$$

then the transverse and longitudinal elastic waves propagate through the solid with the velocities C_{t} and C_{l}, correspondingly (notice that this condition is the generalization of the classic condition (1)). The pressure in the elastic wave is also given by Eq. (1).

When the momentum of atoms

$$p > mC_{\mathrm{a}} \tag{71}$$

a shock wave develops. The temperature-independent time of redistribution of the atoms on the front of shock wave (by means quantum tunnelling in gradient of stress) is

$$\tau_{ij}^{\mathrm{T}} \propto \frac{2a_0}{u}. \tag{72}$$

In the case

$$mC_{\mathrm{a}} > p > mC_{\mathrm{S}}, \tag{73}$$

in consequence of the relations (56) we have

$$\tau_p < \tau_{ij}^{\mathrm{T}} < \tau_{\varepsilon}, \tag{74}$$

and energy of external action is localized in the front of shock wave, that moving with supersonic velocity, D, which is determined by Eq. (2).

By virtue of Eq. (74) the periodicity of crystal lattice has little or no effect on the kinetic of quantum tunneling of atoms in the front of shock wave. Because of this, at the conditions (73) shock wave has a two-wave structure with the elastic precursor.

Here we consider the microscopic expressions for the parameters that determine the kinetics of the various regimes for high-velocity deformation in solids and for shock propagation. In considered above quantum-statistical model of irreversible deformed solid the character of the response for $p > mC_a$ is determined by the parameter

$$Re_{cr} = \frac{L_0}{\xi_0} = \frac{H_0}{C_t^2}, \tag{75}$$

where H_0 is the binding energy of the atoms, ξ_0 is the correlation radius of elastic fields, L_0 is the mean length of relaxation of pulse of atoms in crystal, and the relation

$$\Lambda = L_0/2a_0 = \sqrt{C_t/C_a}$$

is the analog of the De Boer parameter [see, Eq. (21)]. It is pertinent to note that the difference in the behavior of solids for which $Re_{cr} < 1/\sqrt{2}$ and materials with $Re_{cr} > 1/\sqrt{2}$ is analogous to the difference in the behavior of the superconductors of the first and second kinds in a magnetic field (see, for example, Ref. [85]); and the critical parameter Re_{cr} is the analog of the Ginzburg-Landau parameter for superconductors (notice that Re_{cr} is also the analog of the critical value of Reynold's number in hydrodynamics (see Ref. [28]).

As indicated in Refs. [1,2,24,25], for ductile materials

$$Re_{cr} > \tfrac{1}{\sqrt{2}} \sim 0.707, \tag{76}$$

and for brittle materials

$$Re_{cr} < \tfrac{1}{\sqrt{2}}. \tag{77}$$

As is obvious from the data listed in the Tables III and IV, this conclusion is in agreement with the experimental data.

In the case $Re_{cr} > 1/\sqrt{2}$ (ductile materials) macroscopic mass velocity in the elastic precursor u_E and the Hugoniot elastic limit P_{HEL} are given by the equations

$$u_E = C_a, \qquad P_{HEL} = \rho C_a C_l. \tag{78}$$

If the relations (56) are valid an elastic precursor is accompanied by the plastic wave (see, for example, Refs. [2,6,27,86]), Eqs. (78) are in a good agreement with the experiments (see Tables III and IV).

If $Re_{cr} < 1/\sqrt{2}$ (brittle solids) then the deformation of a crystal lattice in the front of shock wave in the case when conditions (73) are valid is dominantly elastic. The Hugoniot elastic limit and the mass velocity for the elastic precursor for brittle material are defined by the following equations:

$$u_E = C_S, \qquad P_{HEL} = \rho C_S C_l, \tag{79}$$

TABLE III. Physico-mechanical properties of plastic materials ($Re_{cr} > 1/\sqrt{2}$) [1,2]. (For an fcc structure, the shortest interatomic distance $r_{ij} = a_0/\sqrt{2}$; for bcc structure, $r_{ij} = a_0\sqrt{3}/2$; and for hexagonal structure, $r_{ij} = a_0$, where a_0 is the lattice parameter).

Material		Al	Ti	Fe	Co	Cu	Pb
r_{ij}, Å		2.022	2.95	2.148	1.775	1.810	2.475
ρ, g/cm^3		2.734	4.5	7.87	8.83	9.02	11.36
$C_a = h/ma$, m/s		26	15	12	11	13	2.75
C_t, m/s		3235	3100	3223	2553	2333	1100
C_l, m/s		6794	6038	5751	5414	4833	2420
$C_S = \sqrt{C_a C_t}$, m/s		290	212	195	168	172	55
$H_0 \times 10^{-3}$, kJ/kg,	experiment	8.2	10.6	7.0	—	5.3	0.85
	experiment	11.9	9.8	7.4	7.3	5.3	0.94
	$C_{cr} \times C_l$	9.5	7.2	6.1	5.3	4.4	0.88
$Re_{cr} = H_0/C_t^2$		1.14	1.1	0.71	1.12	0.93	0.78
C_{cr}, m/s,	H_0/C_l	1750	1620	1287	1348	1000	388
	$\sqrt{C_S C_l}$	1400	1130	1060	955	910	365
P_{HEL}, GPa,	$\rho C_a C_l$	0.48	0.39	0.54	0.53	0.6	0.076
	experiment	0.41	1.0-2.0	0.9-1.4	—	0.8	0.08
	$\rho H_0^4/C_t C_l^5$	1.18	1.3	1.2	1.87	1.26	0.1

TABLE IV. Physico-mechanical properties of brittle materials ($Re_{cr} < 1/\sqrt{2}$) [1,2].

Material		Si	Mo	W	SiC	B_4C	Al_2O_3
ρ, g/cm^3		2,33	10,28	19,3	3,215	2,5	3,99
$H_0 \times 10^{-3}$, kJ/kg,	experiment	16,2	8,65	4.61	20,0	48,0	28,6
	experiment	16,8	7,4	—	—	—	—
C_t, m/s		5510	3355	2904	7906	8957	6401
C_l, m/s		9140	6418	5237	12516	14365	10847
$Re_{cr} = H_0/C_t^2$		0,52	0,6	0,55	0,32	0,6	0,7
C_{cr}, m/s,	H_0/C_l	1840	1040	882	1600	3350	2637
	experiment	—	—	900	1600	—	2500
$(C_a/C_t) \times 10^3$		5,5	2,3	2,6	0,67	7,6	12
$C_S = C_{cr}^2/C_l$		380	160	150	204	782	700
P_{HEL}, GPa,	$\rho C_S C_t$	7,9	10,5	15	8,2	28	30,3
	experiment	7,6	10,0	12	8,3	18	21

where $C_S = \sqrt{C_a C_l}$ is defined by Eq. (50). When $p > mC_S$, the crystal lattice loses stability and the crystal enters a coherent nonequilibrium state (see Fig. 3c). As a result, when

$$mC_S < p < mC_{cr}, \tag{80}$$

TABLE V. Some properties of brittle materials ($Re_{cr} \leq 1/\sqrt{2} \approx 0,707$) [46].

Material	Experimental data				The results of calculation	
	ρ, g/cm^3	C_t, km/s	C_l, km/s	$H_0 \times 10^{-3}$, kJ/kg	C_{cr}, km/s	Re_{cr}
B_4C	2.5	8.95	13.5	48	3.56	0.60
SiC	3.0	7.9	12.5	20	1.60	0.32
SiO_2	2.5	3.07	15.8	9.6	1.85	0.58
Al_2O_3	3.99	6.40	10.85	28.6	2.64	0.70

where

$$C_{cr} = \sqrt{C_S C_l}, \tag{81}$$

according to Eqs. (47), (49) the conditions (48) is valid and, according to Eqs. (56), (72) we have

$$\tau_{ij}^{T} < \tau_p. \tag{82}$$

By these means the momentum of atoms in deformed crystal is fixed and by virtue of the Heisenberg's uncertainty principle a one-to-one correspondence between the number of atoms N_a and the number of sites on a lattice N_0 is violated. In turn, the delocalized atoms fill the band of mobility. Energy spectrum of atoms of solid which deformed in regime (80) is shown on the Fig. 3c. As a result, if the conditions (80) are valid the ductile crystalline solid ($Re_{cr} > 1/\sqrt{2}$) is deformed hydrodynamically (but in the nonstationary regime); while brittle solids ($Re_{cr} < 1/\sqrt{2}$) experience multiple fracture. The difference in the behavior patterns of brittle and plastic solids in regime (80) is analogous to the difference in the behavior patterns of superconductors of the first and second kinds in a magnetic field H in the case $H_{C1} < H < H_{C2}$, where H_{C1} and H_{C2} are the lower and upper critical fields.

It is easy to show (see Refs. [1,25]) that C_{cr} is the limiting velocity of crack propagation in atomic crystal lattice. This velocity is also equal to

$$C_{cr} = \frac{H_0}{C_l}. \tag{83}$$

As one might see from comparisons between the experimental and theoretical values of P_{HEL}, C_S and C_{cr}, which appear in Tables IV and V, the results of analytical calculations by means Eqs. (78)–(83) agree well with the experimental data.

When $u > C_{cr}$, an induced energy gap opens in the mobility band (see Fig. 3d). Thus, if

$$mC_{cr} < p < mC_l, \tag{84}$$

then both plastic and brittle solids behave like quantum crystals (see, for example Refs. [54–56], and Eqs. (21), (29), (30)). It is well known that under certain conditions

(including high pressure and high deformation velocities, which are realized, for example, during explosive welding and during the formation of a cumulation jet, see Refs. [6,34]), a solid flows as liquids do, while remaining in a crystalline state. This flowing state of a solid, observed in regimes (80) and (84) for plastic solids and only in regime (84) for brittle materials, however, is not characterized by the complete absence of an increase in the tangential stresses upon an increase in the shear deformations. That is, beginning at certain critical shear strains and stresses the solid stops opposing further increase in the shear, going into a hydrodynamic deformation regime (84). If the Reynold's number of the flow $Re = ud/\nu$ is smaller then Re_{cr}, where d is the characteristic size of the flow and the viscosity is

$$\nu = C_t^2 \tau_p = 2a_0 C_t \Lambda^2, \tag{85}$$

then the deformation of solid in hydrodynamic regime (84) is laminar, and for

$$Re > Re_{cr} \tag{86}$$

it is turbulent in character. This also applies to regime (80).

In the case

$$p > mC_l, \tag{87}$$

the ductile solid $Re_{cr} > 1/\sqrt{2}$) in the front of the shock wave becomes liquid (when $p < mC_l$ the material melts only in the stress relief wave) as a result of the quantum tunnel melting in a resonance pressure gradient. This effect is similar to the gigantic stimulation of tunnel processes by a resonant electromagnetic field examined by Ivlev [87]. This conclusion has been confirmed experimentally [88].

5. APPLICATION OF QUANTUM-STATISTICAL APPROACH TO SOME PROBLEMS OF ARMOR PIERCING

Below we consider the application of quantum-statistic model to the problems of high-velocity penetration of long rods into solid targets which were discussed in Sect. 1.2.

In the problem of the high-velocity impact of solids, as in any other dynamic problem, the main question concerns the forces that characterize motion, that is, the forces that determine the resistance to penetration. Upon the interaction of solid bodies at velocities that exceed the velocities of defects propagations, one can expect that the resistance of a target material to the penetration of a projectile should determined by the strength parameters of an impact-loader body that are dependent on the physicochemical nature and on the structural parameters of the target material. Evidently, the impact velocities of solids should be on the order of magnitude of the velocity of sound in the material studied, *i.e.*, 10^3–10^4 m/s. Keeping in mind this range of interaction velocity, let us turn to a brief analysis of the models available of the high-velocity impact of solids.

The key question is how the strength term for the target depends on the material properties of the target. The use of a quantum-statistic model of a dynamic deformation

TABLE VI. Comparison of results of calculations of penetration velocity of copper rod into targets made of brittle material with experimental data (see Ref. [46]).

Material of target	Impact velocity v_0, km/s	Penetration velocity, u, km/s		
		The results of calculation by Taylor's formula (5)	Experimental data (Zlatin, Kozushko)	The results of calculation by Balankin's formula (88)
B_4C	8.1	5.3	3.85	3.90
SiC	7.55	4.8	3.60	3.60
SiO_2	5.25	4.44	3.0	3.1
Al_2O_3	7.15	4.29	3.75	3.8
	5.90	3.54	2.83	3.1

of a solid makes it possible to obtain the relation determining the penetration velocity and depth of penetration of an elongated metal rod in a solid target without any adjustable parameters. In the turbulent hydrodynamic regime (84), (86) of deformation of the rod and the target, the penetration velocity in the stationary stage is equal to

$$u = \frac{\beta^2 v_0}{1-\beta^2}\left[1 - \sqrt{1-(\beta^2-1)(Z^2-1)}\right], \tag{88}$$

where

$$\beta = \sqrt{\frac{\rho_r[1+2(Re_{cr}^r)^{-1}]}{\rho_t[1+2(Re_{cr}^t)^{-1}]}}, \tag{89}$$

$$Z^2 = 2\,\frac{\rho_t(C_{cr}^t)^2 - \rho_r(C_{cr}^r)^2}{\rho_r[1+2(Re_{cr}^r)^{-1}]v_0^2}. \tag{90}$$

Here indices r and t refer to the rod and target, respectively, and parameters Re_{cr} and C_{cr} are defined by Eqs. (75) and (81) or (83).

In Table V the values of the velocities of longitudinal and transverse elastic waves and heat of atomization for some materials are listed. The results of comparing calculations using the proposed Eqs. (88)–(90) and (78)–(83), with experimental data on the high velocity penetration of long rods into targets made from various materials are given in Table VI. We can see that there is very good agreement between the theoretical values of penetration velocity and the experimental data, given that the scatter in the values of H_0, C_l and C_t in the literature is incomparably less than the scatter in the experimental values for the limiting crack velocity C_{cr} and the Hugoniot elastic limit P_{HEL}. The solutions for other regimes of high velocity deformation of materials of target and rod can be obtained in a similar manner (see, for example, Refs. [1,2,5,6]).

6. CONCLUSIONS

As we have shown, knowing the elastic properties, matter density and heat of atomization it is possible to predict the shock strength and dynamic behavior of brittle and ductile materials, with an accuracy adequate for experiments.

Moreover, quantum statistical approach can be used to obtain microscopic expressions for the parameters in the models of explosive, high voltage electrical discharge, and friction welding of metals (see Refs. [89]), of spalling phenomena (proposed in Ref. [90]), of the process of mechanical alloying (developed in Refs. [91–93]), of compaction of metal powders using high voltage electrical discharge (see Refs. [89,94]), for the super-deep penetration phenomenon (considered in Refs. [1,45,95]), and in other cases as well.

However quantum statistical approach is applicable not only to dynamic problems of solid mechanics but also to some quasi-static problems such as creep of ideal crystals and amorphous materials (see Eqs. (57) and (64)-(69)), superplasticity phenomenon (see Ref. [96]), to the description of phase transformations of a crystal solid (see Refs. [1,2,97]), to developing a theory of plastic deformation of ceramic at low temperature (see Ref. [98]), to the formulation of quantum statistical models of chemical reactions in solid phase (see Refs. [89]), to the determination of the parameters that govern the electron fracture mode in solids [99], to the description of the brittle-ductile kinetic transition in the kinetics of metal fracture [58], and for the determination of strength parameters that govern the processes of fracture of nanostructural materials (see Ref. [100]).

Furthermore, we believe that further developments of the approach reviewed make it possible to create microscopic theories of such phenomena as shock synthesis of diamonds (see Ref. [89]), high temperature self-accelerated synthesis (see Ref. [89]), electro stimulation of plastic deformation of metals (see Ref. [101]), which are of great importance in advanced metallurgical technologies considered in Refs. [16,89].

ACKNOWLEDGMENTS

The author is grateful to Professor Gennady Cherepanov (Florida International University) for useful discussions. The courtesy and support of the staff and faculty of Material Research Program at ITESM-CEM and especially the Chairperson Professor Armando Bravo, are gratefully acknowledged.

REFERENCES

1. A.S. Balankin, *Synergetics of Deformed Solids*, Department of Defence USSR Press, Moscow (1991).
2. V.B. Lazarev, A.S. Balankin, A.D. Izotov and V.B. Kozhushko, *Structural Stability and Dynamical Strength of Inorganic Materials*, Nauka, Moscow (1993).
3. F.A. Baum, L.P. Orlenko, K.P. Stanukovich, V.P. Chelyshev and B.I. Shehter, *Physics of Explosion*, Nauka, Moscow (1975).
4. J. Sternberg, *J. Appl. Phys.* **65** (1989) 3417.
5. A.S. Balankin, A.A. Lyubomudrov and I.T. Sevryukov, *Kinetic Theory of Cumulative Armor-Piercing*, Department of Defence USSR Press, Moscow (1989).

6. A.S. Balankin, A.A. Lyubomudrov and I.T. Sevryukov, *The Physics of High Velocity Impact*, Department of Defence USSR Press, Moscow (1990).
7. G. Cherepanov, *Mechanics of Brittle Fracture*, McGraw Hill, New York (1979).
8. J. Rice and R. Thomson, *Philos. Magazine* **29** (1974) 73.
9. V. Lazarev, A.S. Balankin and A.D. Izotov, *Inorganic Materials* **29** (1993) 909.
10. A.S. Balankin, A.D. Izotov and V. Lazarev, *Inorganic Materials* **29** (1993) 375.
11. A.D. Izotov, A.S. Balankin and V. Lazarev, *Inorganic Materials* **29** (1993) 769.
12. A.S. Balankin and P. Tamayo, *Rev. Mex. Fís.* **40** (1994) 506.
13. G. Cherepanov, *Problems of Strength* **N2** (1989) 3.
14. M. Born and K. Huang, *Dynamical Theory of Crystal Lattices*, Clarendon, Oxford (1954).
15. T.L. Anderson, *Fracture Mechanics: Fundamentals and Applications*, CRC Press, Boston (1991).
16. V.S. Ivanova, A.S. Balankin, L. Bunin and A. Oksogoev, *Synergetics and Fractals in Material Science*, Nauka, Moscow (1994).
17. A.S. Balankin and A. Bugrimov, in *Abstr. XXVIII Int. Congr. of Theor. and Appl. Mech.*, Haifa, Israel, August 22–28, 1992, IUTAM Press: Haifa (1992) p. 175.
18. A.S. Balankin, *Sov. Phys. Solid State* **34** (1992) 658.
19. A.S. Balankin, *Transl.: Doklady of the USSR Academy of Science: Earth Science Sections* **319 A** (1993) 29.
20. A.S. Balankin, *Doclady Academy of Science Russia* **322** (1992) 869.
21. A.S. Balankin and V.S. Ivanova, *Sov. Tech. Phys. Lett.* **17** (1991) 12.
22. A.S. Balankin, *Sov. Tech. Phys. Lett.* **16** (1990) 248.
23. A.S. Balankin, *News of Academy of Science Russia, ser.: Metals* **N2** (1992) 41.
24. A.S. Balankin, *Sov. Phys. Tech. Lett.* **17** (1991) 531.
25. A.S. Balankin, *Sov. Tech. Phys. Lett.* **15** (1989) 878.
26. A.S. Balankin, *Sov. Tech. Phys. Lett.* **14** (1988) 540.
27. A.L. Fetter and J.D. Walecka, *Theoretical Mechanics of Particles and Continua*, McGraw-Hill, New York (1980).
28. L.D. Landau and E.M. Lifshitz, *Fluid Mechanics*, Pergamon Press, Oxford (1979).
29. W.C. Moss, *J. Appl. Phys.* **55** (1988) 540.
30. L.V. Alshuler and B.S. Chekin, *Appl. Mech. and Theor. Phys.* **1** (1988) 119.
31. D.J. Steinberg, S.G. Cochran and H.W. Guinan, *J. Appl. Phys.* **51** (1980) 320.
32. A.A. Kozhushko, A.D. Izotov, V. Lazarev and A.S. Balankin, *Inorganic Materials* **29** (1993) 1171.
33. A.A. Kozhushko, A.D. Izotov, V. Lazarev and A.S. Balankin, *Inorganic Materials* **29** (1993) 1189.
34. G. Birkhoff, D. Dougall, E. Pugh and G. Taylor, *J. Appl. Phys.* **19** (1948) 563.
35. M.A. Lavrentev, *Progress in Mathemat. Sci., USSR* **12** (1957) 41.
36. W.A. Allen and J.W. Rodgers, *J Franklin Inst.* **272** (1961) 275.
37. R. Kinslow (editor), *High-Velocity Impact Phenomena*, Academic Press, New York (1970).
38. A. Ya. Sagomonian, *Penetration*, Moscow University Press, Moscow (1974).
39. G. Solve and J. Caguoux, *Bull. Am. Phys. Soc.* **34** (1989) 1714.
40. A.A. Kozhushko, I.I. Rykova and A.E. Sinani, *J. de Physique* **1** (1991) C3-117.
41. A. Tate, *J. Mech. Phys. Solids* **15** (1967) 387.
42. N.A. Zlatin and A.A. Kozhushko, *Sov. Phys. Tech. Phys.* **27** (1982) 212.
43. S.A. Kinelovskii and B.E. Maevskii, *Zh Prikl. Mekh. Tech. Fiz.* **N2** (1989) 150.
44. A.S. Balankin and G.N. Yanevich, *Sov. Phys. Tech. Phys.* **37** (1992) 625.
45. A.S. Balankin and G.M. Yanevich, *Sov. Tech. Phys. Lett.* **17** (1991) 236.
46. A.S. Balankin, S.V. Levin and G.N. Yanevich, *Sov. Phys. Tech. Phys.* **37** (1992) 339.
47. A.S. Balankin, A.A. Lyubomudrov and I.t. Sevryukov, *Sov. Phys. Tech. Phys.* **34** (1989) 1431.

48. A.S. Balankin, A.A. Lyubomudrov, I.T. Sevryukov and G.N. Yanevich, *Sov. Tech. Phys. Lett.* **14** (1988) 537.
49. A.S. Balankin, *Sov. Tech. Phys. Lett.* **14** (1989) 534.
50. A.S. Balankin, *Sov. Phys. Tech. Phys.* **33** (1988) 1107.
51. A.S. Balankin, *Sov. Phys. Tech. Phys.* **33** (1988) 1452.
52. A.S. Balankin, *Combustion, Explosion Shock Waves (USSR)* **N 4** (1989) 130.
53. A. Kozhushko and V. Maiboroda, *Shock Compression of Condensed Matter*, S. Schmidt, R. Dick, J. Forbes and D. Tasker (editors), Elsevier Science Publisher, New York (1988) 959.
54. A.M. Kosevich, *Physical Mechanics of Real Crystals*, Naukova Dumka, Kiev (1981).
55. M. Bretz, J.G. Dash, D.S. Hickernell, E.O. McLean and O.E. Vilches, *Phys. Rev.* **A 8** (1973) 1589.
56. A.F. Andreev, *Sov. Phys. Usp.* **19** (1976) 137.
57. A.Z. Patashinskii and B.I. Shumilo, *Sov. Phys. JETP* **62** (1985) 177.
58. A.S. Balankin, V.S. Ivanova and V.P. Breusov, *Sov. Phys. Dokl.* **37** (1992) 105.
59. A.S. Balankin, *Sov. Phys. Dokl.* **37** (1992) 379.
60. A.S. Balankin, *Sov. Tech. Phys. Lett.* **17** (1991) 229.
61. V.P. Dmitriev, *Sov. Phys. Dokl.* **32** (1987) 135.
62. M.T. Sprackling, *The Plastic Deformation of Simple Ionic Crystals*, Academic Press, London (1976).
63. L.D. Landau and E.M. Lifshitz, *Statistical Physics*, Part 2, Pergamon Press, Oxford (1978).
64. J. Hubbard, *Proc. Roy. Soc.*, London **A276** (1963) 238.
65. A.B. Harris and R.V. Lange, *Phys. Rev.* **157** (1967) 295.
66. P.W. Bridgman, *Studies in Large Plastic Flow and Fracture, with Special Emphasis on the Effects on Hydrostatic Pressure*, McGraw-Hill, New York (1952).
67. B.B. Mandelbrot, *The Fractal Geometry of Nature*, W.H. Freeman and Company, New York (1983).
68. V.E. Panin (editor), *Structural Levels of Plastic Deformation and Fracture*, Nauka, Novosibirsk (1990).
69. C.W. Chan, *Physical Metallurgy*, North Holland, Amsterdam, (1970).
70. G.F. Lepin, *Metal Creep and Criteria for High-Temperature Strength*, Metallurgiya, Moscow (1976).
71. A.S. Argon, *Constituve Equations in Plasticity*, The MIT Press, Cambridge (1975).
72. V.R. Regel, A. Slutsker and S. Tomashevskii, *The Kinetic Nature of the Strength of Solids*, Nauka, Moscow (1974).
73. W. Koster and H. Franz, *Met. Rev.* **6** (1961) 1.
74. M.A. Sadovskii and V.F. Pisarenko, *Seismic Process in Block Media*, Nauka, Moscow (1991).
75. A.S. Balankin, *Sov. Phys. Solid State* **24** (1982) 2102.
76. V.F. Elesin and A.S. Balankin, *Sov. Phys. Solid State* **28** (1986) 372.
77. A.A. Alexandrov, A.S. Balankin and A.E. Parshakov, *Sov. J. Low. Temp. Phys.* **13** (1987) 321.
78. A.S. Balankin, *Sov. J. Low. Temp. Phys.* **14** (1988) 187.
79. A.S. Balankin and E.S. Balankina, *News of Acad. Science USSR, ser. Metals* **N 1** (1990) 140.
80. H. Haken, *Information and Self-Organization. A Macroscopic Approach*, Springer-Verlag, New York (1990).
81. J. Feder, *Fractals*, Plenum Press, New York (1989).
82. A.S. Balankin and A. L. Bugrimov, *Polymer Science USSR* **34** (1992) 246.
83. V.I. Gorobets and L.Zh. Gorobets, *New Trends in Research on Grinding*, Nedra, Moscow, (1977).
84. I.S. Sokolnikoff and R.M. Redheffer, *Mathematics of Physics and Modern Engineering*, McGraw-Hill, New York (1966).
85. P. De Gennes, *Superconductivity of Metals and Alloys*, Springer-Verlag, New York (1965).

86. H. Kolsky, *Stress Waves in Solids*, Dover Publications, New York (1963).
87. B.I. Ivlev, *JETP Lett.* **41** (1985) 142.
88. B.S. Chekin, *Prikl. Mekh. Theor. Fiz.* **N 2** (1978) 89.
89. A.S. Balankin, "Advanced Technologies of Material Treatment" in *News of Science and Technology, Ser.: New Materials and Technologies of Their Creations and Treatments,* **N 2** Academy of Science USSR Press, Moscow (1991).
90. V.A. Meshcheryakov, *Sov. Phys. Tech. Phys.* **33** (1988) 381.
91. A.S. Balankin, V.S. Ivanova, A.A. Kolesnikov and E.E. Savitskaya, *Sov. Tech. Phys. Lett.* **17** (1991) 504.
92. V.S. Ivanova, A.S. Balankin, V. Ermishkin, Y. Kovneristyi and P. Tamayo, *Sov. Phys. Dokl.* **37** (1993) 222.
93. A.S. Balankin and A.A. Kolesnikov, "Mechanical Alloying" in *News of Science and Technology, Ser.: New Materials and Technologies of Their Creations and Treatments,* **N 9** Academy of Science USSR Press, Moscow (1991).
94. S.A. Balankin, N.P. Stepanov and A.V. Hripko, *Compaction of Metal Powders Using High Voltage Electrical Discharge*, Electronica Press, Moscow (1986).
95. G.P. Cherepanov, *Eng. Fract. Mech.* **47** (1994) 691.
96. V.V. Rybin and V.N. Perevezentsev, *Sov. Tech. Phys. Lett.* **7** (1981) 515.
97. A.S. Balankin, *Sov. Phys. Solid State* **24** (1982) 1977.
98. J. Karch, R. Birringer and H. Gleiter, *Nature* **330** (1987) 556.
99. G.P. Cherepanov, A. Borzykh, *J. Appl. Phys.* **74** (1993) 7134.
100. G.P. Cherepanov, A.S. Balankin and V.S. Ivanova, accepted for publication in *Eng. Fract. Mech.* (1995).
101. V. Ivanova, A.S. Balankin and O.A. Bannih, *Metals* **N 2** (1992) 11.